METALS AND MATERIALS, Vol. 2, No. 2 (1996), pp. 81~91

Effect of Minor Elements on Hot Cracking Susceptibility of Austenitic Stainless Steel Welds

Chang Hee LEE

Department of Metallurgical Engineering and
Research Institute of Steel Process and Application
Hanyang University, 17 Haengdang-Dong, Seongdong-Ku, Seoul 133-791, Korea

This research evaluates the effects of Si, N and REM on the hot cracking behavior of specially designed austenitic stainless steels. Varestraint hot cracking tests and microstructural examination revealed that solidification cracking of 304 can be minimized by a suitable addition of Si, N and control of the solidification mode. Further, the addition of N to "fully" austenitic 316 weld metal decreased solidification cracking susceptibility. REM additions were also effective in reducing solidification and weld metal HAZ liquation cracking in 347, but was ineffective for reduction in base metal HAZ liquation cracking.

1. INTRODUCTION

It is generally considered that silicon is harmful from the hot cracking stand point in stainless steels. The influence of silicon is, however, known to be different in weld metals with different chemical compositions. When the material has a fully austenitic composition, hot cracking is more sensitive to silicon content, whereas a partially ferritic composition is not as sensitive and Si can be tolerated up to 1.5-2.5% without any detrimental effect on hot cracking susceptibility [1].

Nitrogen, in general, is also known to decrease the hot cracking susceptibility of low ferrite austenitic stainless steels, simply because of its effect on the solidification mode (tendency toward primary or full austenite) and thus reduced ferrite potential. Nevertheless, the addition of nitrogen to low carbon grade stainless steels to compensate for the strength reduction brought about by the reduced carbon content for lower intergranular corrosion (sensitization) has been accomplished without detrimental effects. Nitrogen additions have been linked to improved corrosion resistance, a more or less fortuitous effect. Further, it is known that nitrogen can be tolerated if the elemental balanced is adjusted so as to ensure a primary ferritic solidification mode which will provide residual ferrite in the room temperature microstructure. Recent research works by Ogawa *et al.* [2] and Chou *et al.* [3] indicate that some addition of nitrogen to fully austenitic stainless steel welds resulted in a reduced solidification cracking and heat affected zone (HAZ) liquation cracking susceptibility.

Rare earth metals (REM, a mixture of La, Ce, Nd, etc.) are used for desulfurization and sulfide shape control in iron and steel making [4-7], due to the strong deoxidizing potential of REM. Recently, a number of Japanese researchers [8, 9] have investigated the potential beneficial effect of REM on solidification cracking in austenitic stainless steels. Matsuda *et al.* [9] have found that a La or REM addition improved solidification cracking resistance of 310, a fully austenitic stainless steel. The main reason for the beneficial effect was the formation of high melting point La or REM containing phosphides and sulfides as opposed to the formation of lower melting MnS type sulfides and M_3P type phosphidesin austenitic stainless steel welds. Morishige *et al.* [8] have also recommended the addition of REM up to 0.02% in 347 to improve hot ductility and resistance to the fusion zone cracking.

This paper includes evaluation of the effects of Si and its synergistic effects with N on the hot cracking propensity of austenitic stainless steel welds. Further, two heats of type 347 with REM additions have been evaluated and compared to that of a heat of AISI 347 (similar chemical composition except for REM additions). The weld fusion zones were constituted to have different levels of the added element while maintaining all other elements at a constant level by using "the element implant technique" or by obtaining materials with different lev-

Table 1. Chemical compositions of the materials evaluated in this study

Code	Type	C	Si	Mn	P	S	Cr	Ni	Mo	N	Nb	Co	Cu	N	V	FN[a]	FN[b]	REM[c]
347-5	347L	0.030	0.17	1.61	0.013	0.007	18.58	11.49	-	-	0.30	-	-	-	-	0.0	0.0	0.008
347-6	347R	0.020	0.51	1.43	0.019	0.012	18.22	10.14	-	-	0.74	-	-	-	-	3.5	3.0	0.017
347-9	AISI 437A	0.037	0.63	1.56	0.029	0.001	18.00	9.67	0.32	0.044	0.61	-	-	-	-	3.0	5.0	-
304Si-A	304	0.015	0.54	1.43	0.026	0.008	18.19	9.17	0.29	0.078	-	-	-	-	-	3.0	-	-
304Si-A	304	0.032	0.78	1.32	0.026	0.008	18.19	9.17	0.29	0.078	-	-	-	-	-	4.0	-	-
304Si-C	304	0.050	1.25	1.25	0.026	0.008	18.19	9.17	0.29	0.078	-	-	-	-	-	8.0	-	-
316N-A	316	0.042	0.34	3.23	0.016	0.012	17.59	13.80	2.15	0.047	0.01	0.07	0.35	0.047	0.11	0.0	-	-
316N-B	316	0.040	0.33	3.12	0.016	0.012	17.64	13.80	2.15	0.078	0.01	0.07	0.32	0.078	0.11	0.0	-	-
316N-C	316	0.041	0.29	3.08	0.016	0.011	17.62	13.78	2.15	0.120	0.01	0.08	0.26	0.12	0.11	0.0	-	-

a: Measured ferrite content with magne-gage.
b: Ferrite potential by Delong method.
c: Rare earth metals

els of specific elements.

2. MATERIALS AND EXPERIMENTAL PROCEDURES

2.1. Materials and sample preparation

Materials evaluated in this study include AISI 304, 316 and 347 austenitic stainless steels. The chemical composition and the ferrite content measured on the autogenously fused zone are given in Table 1.

In order to modify the silicon content in the fusion zone of 304, the element implant technique, using an Fe-3.5%Si alloy was employed. The modified chemical composition with three different levels of Si are given in Table 1. The silicon content varies from 0.54% to 1.25%.

Further, in order to investigate the synergistic effect of Si with N, the highest Si implanted samples (1.25%) were subsequently fused under a N_2 containing Ar shielding gas. The various N levels in the fusion zone were obtained by the addition of a different volume percent of nitrogen (0, 5%, 20%) to the Ar shielding gas during autogenous welding. Since this technique involves the addition of N_2 to the shielding gas, the basic composition of the fused zone was not changed. However, the ferrite content and solidification mode is altered depending on the amount of the N_2 addition.

To further evaluate the effects of N, three different nitrogen containing type 316 electrodes were deposited by the shielded metal arc welding (SMAW) as shown schematically in Figure 1. The welding conditions were; 160 A, 24V, and 25.4 cm/min travel speed. The chemical composition of the as-deposited weld metals are given in Table 1. Nitrogen content varies from 0.047% to 0.12%. The major and minor alloying elements are almost constant for the three welds. The ferrite content measured with Magne-Gage revealed that, as planned, all three weld metals were fully austenitic. Four Varestraint samples were extracted from each weld deposit for hot cracking evaluations.

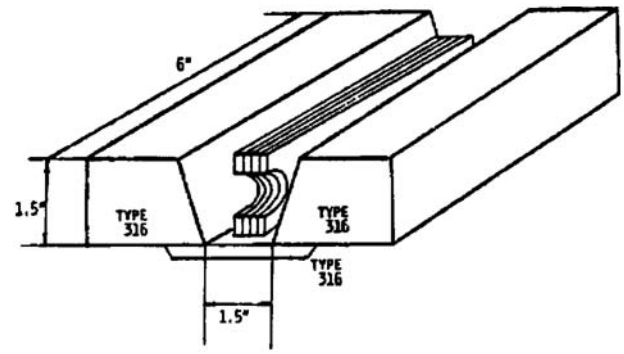

Fig. 1. A schematic drawing of a groove weld deposited with three different N containing electrodes (SMAW) from which Varestraint samples were extracted.

2.2. Experimental procedures

2.2.1. Element implant technique

In the implant technique, as shown in Figure 2, a thin sheet of material with the desired element content (in this case Fe-3.5%Si) was cut to the appropriate size (to provide the desired composition in the fusion zone) and spot welded to the test specimen. An autogenous gas tungsten arc (GTA) weld was made to fuse the implant material and combine it with the base metal. With the knowledge of the chemical composition of the added material, the base material and the fusion zone cross section, the desired composition can be obtained.

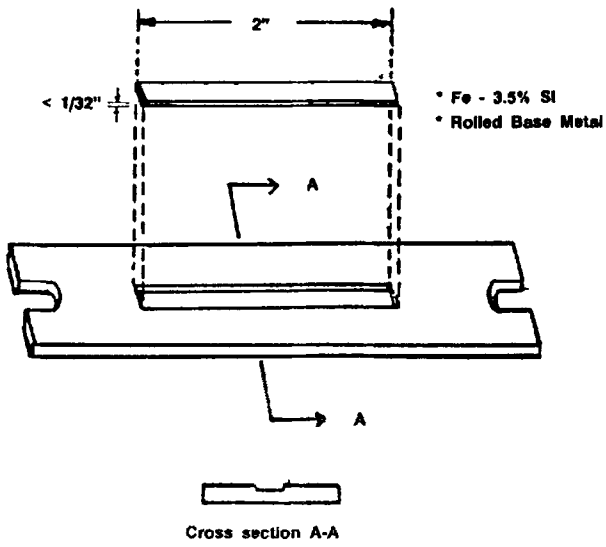

Fig. 2. Schematic representation of the element implant technique.

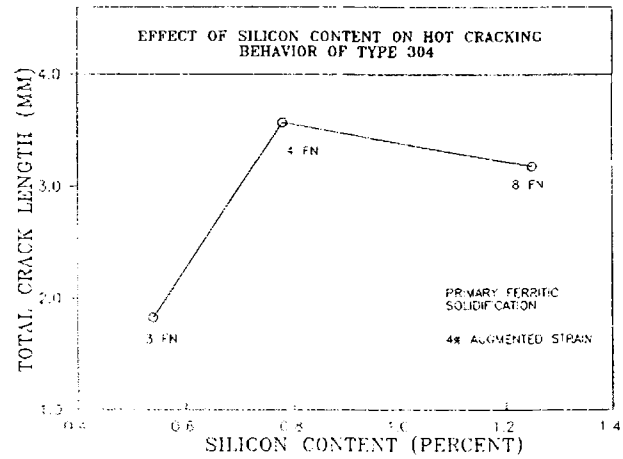

Fig. 3. Effect of silicon content on solidification cracking in 304.

2.2.2. Varestraint hot cracking test (multipass technique)

Testing for hot cracking susceptibility of materials was conducted using the standardized Varestraint method modified in terms of testing concept and design. The main concept changes involve a multipass technique which provides for a simultaneous evaluation of hot cracking susceptibility of the fusion zone, weld metal HAZ and base metal HAZ using the same specimen.

The testing conditions and proceeding are given in elsewhere [10, 18].

The range of augmented strains used in this study was 0-4%. The crack length was measured on the as-welded surface using a binocular microscope at a magnification of 70X. For comparison, the maximum crack length (MCL), total crack length (TCL) and cracking threshold strain for each of the weld zones were measured and recorded.

2.2.3. Microstructural examination

Microstructural examination of selected samples was conducted by optical light microscopy ad SEM after etching in diluted aqua-regia (1 part nitric acid, 3 parts of hydrochloric acid and 1 part of distilled water).

Thin metal discs extracted from the weld metal in a direction perpendicular to the welding direction were used for transmission electron microscope (TEM) and carbon extraction replicas were analyzed using the scanning transmission electron microscope (STEM). The thin foils were prepared using ion milling (Gaton Duomill-Model 6000) under a two beam condition with an angle of 15° at 6 kV and 1 mA of total current (each beam at 0.5 mA)

3. RESULTS AND DISCUSSION

3.1. Si and its synergistic effects with N

The effect of silicon on solidification crack susceptibility of type 304 stainless steel is illustrated in Figure 3. In this figure, the total crack length is plotted as a function of the silicon content. Each data point is the average of three tests at 4% augmented strain. Figure 3 clearly indicates that as Si increases to 0.78%, the susceptibility to solidification cracking also increases. When the Si content is greater than 0.78%, no further increase in the extent of cracking can be noted. In fact, when the Si increased to 1.25%, the extent of cracking decreases slightly as compared to that at 0.78%Si. However, the cracking susceptibility is still greater than that at 0.54%Si. All materials have a primary ferritic solidification mode and the ferrite content increases as the silicon content increases due to the strong ferrite stabilizing effect of Si. As the Si increased to 0.78%, there was almost no change in FN. However, when the Si content reached 1.25%, the room temperature residual ferrite content more than doubled (8 vs. 3 FN). The slightly decreased solidification cracking in the high Si (1.25%) sample as compared to the 0.78 %Si sample may be due to an increased amount of primary ferrite during solidification (increased Cr_{eq}/Ni_{eq}) and thus concomitantly higher room temperature ferrite content.

The typical microstructure and crack morphology in the 1.25%Si weld metal is shown in Figure 4a. Cracking has occurred along solidification grain boundaries, along

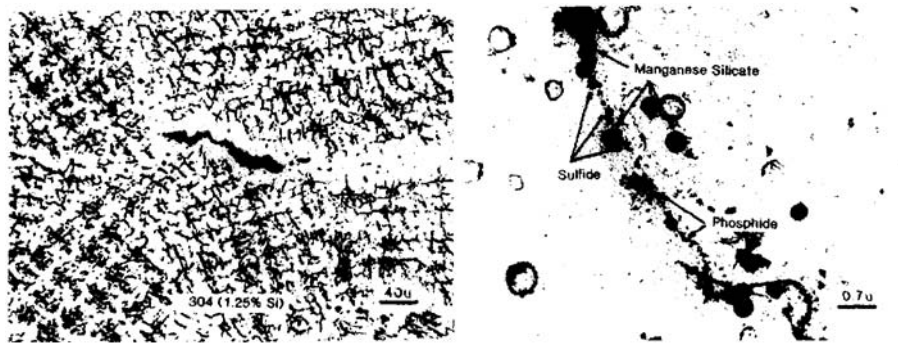

Fig. 4. Typical solidification crack in the 1.25%Si containing 304. a) optical micrograph and b) TEM (carbon extraction replica)

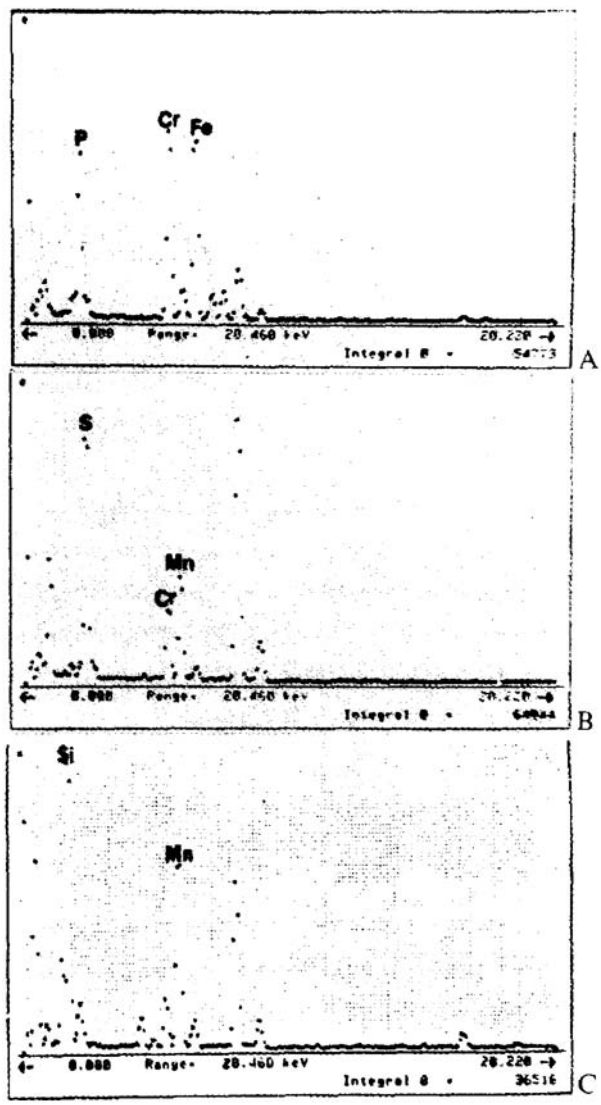

Fig. 5. STEM analysis of a) phosphide, b) sulfide and c) manganese silicate.

which a significant amount of silicates, phosphides and

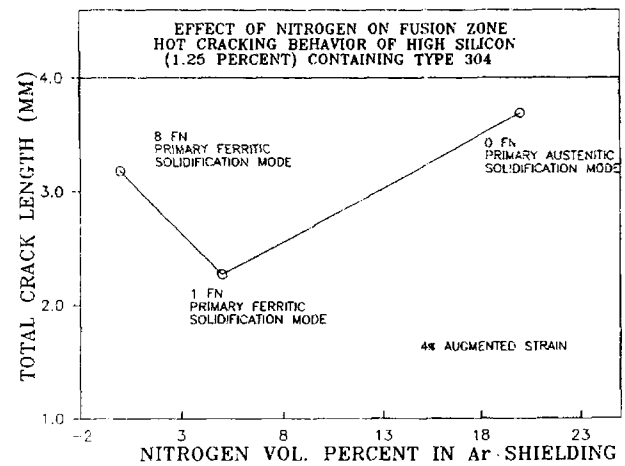

Fig. 6. Effect of nitrogen addition on solidification cracking in the high Si containing 304 (1.25%).

sulfide have precipitated, as shown in the TEM micrograph from the carbon extraction replica in Figure 4b. Figure 4b reveals that the solidification grain boundary is continuously decorated by the fine sulfides, phosphides and larger manganese silicates (STEM analysis on these particles is given in Figure 5. Therefore, the greater solidification cracking susceptibility of the higher Si alloy appears to be directly associated with segregation of Si in addition to S and P, which in turn form low melting silicates, sulfides and phosphides in the grain boundaries.

The effect of nitrogen additions on fusion zone hot cracking behavior of the high Si containing (1.25%) 304 weld metal is shown in Figure 6. The total crack length is plotted as a function of the volume percent N2 in the Ar shielding gas. When 5% nitrogen was added to the Ar shielding gas, the TCL (unexpectedly), decreased as compared to the 100% Ar weld. However, when the nitrogen was increased to 20 vol%, the extent of cracking

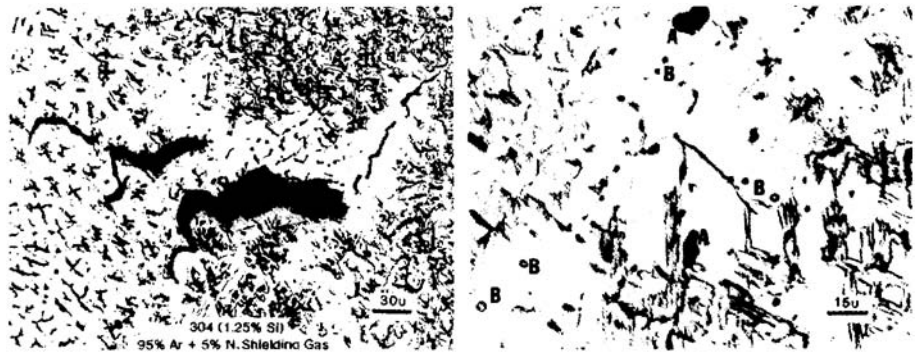

Fig. 7. Solidification cracks in the primary ferritic high Si (1.25%) weld metal, 5%N_2+95%Ar.

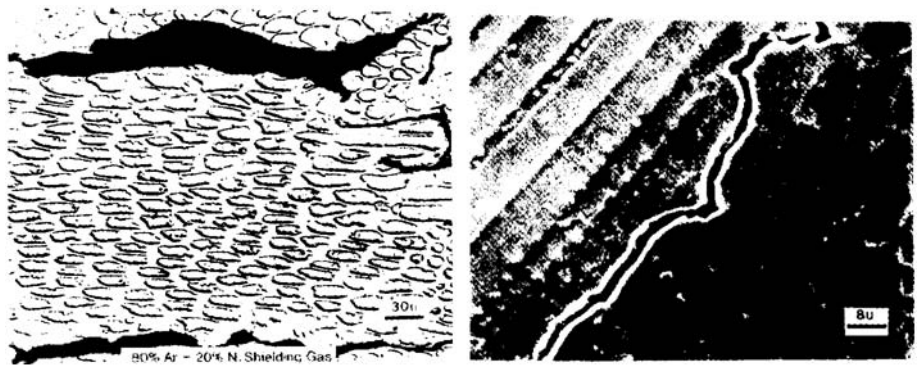

Fig. 8. Solidification cracks in the fully austenitic high Si (1.25%) weld metal. 20%N_2+80%Ar.

again increased significantly. The room temperature microstructures for both the 5 vol% and 20 vol% additions are shown in Figures 7 and 8, which reveal that the 5 vol% N_2 addition exhibits a primary ferritic solidification mode and about 1 FN retained ferrite. On the other hand, the 20 vol% N_2 addition resulted in a solidification mode change from the primary ferritic to fully austenitic. Thus, the significant increase in cracking in the fusion zone when welded with the 20 vol% N_2 shielding gas is mainly due to fully austenitic solidifcation, which results in an increase in segregation of low melting temperature phosphides and sulfides along the dendritic boundaries as shown in Figure 8b.

As long as the weld metal maintains the primary ferritic solidification mode, the addition of N does not appear to have a harmful effect on cracking susceptibility. In fact, the extent of cracking of the high silicon containing 304 (1.25%) decreased. A very similar result was reported by a Russian researcher [12], in that an increase in the nitrogen content did not exert harmful effects on hot cracking susceptibility of the weld metal having a ferrite-austenite mixed microstucture. Other Russian researchers [11] have found that when nitrogen is added to the weld metal, the permissible silicon content without causing solidification cracking is raised. The hot cracking susceptibility of the 0.4-0.45%Si containing alloy was decreased by increasing the nitrogen content to 0.1-0.12%. However, if the Si concentration is further increased (beyond a critical amount), the susceptibility to cracking decreases. These researchers attributed the increased resistance of the nitrogen containing weld metal to the retardation of the polygonization process by the nitrogen atoms. Ogawa *et al.* [2] have also found that the addition of nitrogen has lowered hot cracking susceptibility of the high silicon unstabilized fully austenitic weld metal. They attributed the beneficial effect to the fact that the nitrogen addition may inhibit the enrichment of silicon at grain boundaries.

A careful examination of Figure 7b reveals two other second phases in addition to the sulfides and phosphides; type A phase is relatively large and has a blocky morphology, in contrast to type B phase which is small and has a globular morphology with a bright appearance. The STEM analysis of these particles in Figure 9 reveals that both phases are basically Si-Mn oxides (silicates). However, the type B silicate contains a significant amount of S. As shown before, in the 1.25 %Si weld metal fused with 100% Ar shielding gas, only the type A

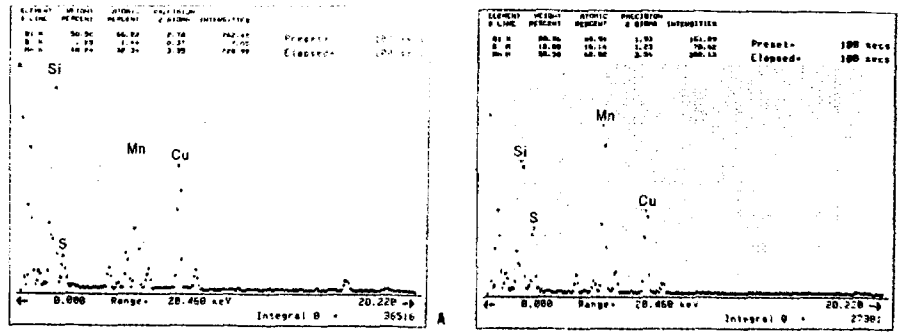

Fig. 9. STEM analyses on manganese silicates a) type A and b) type B.

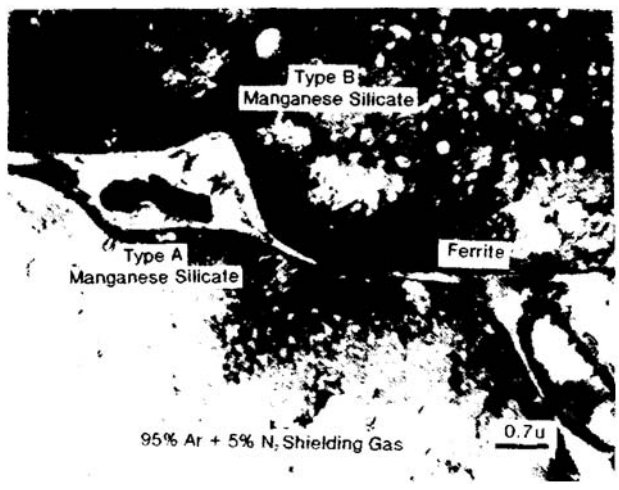

Fig. 10. Typical TEM micrograph of the high Si and N containing primary ferritic 304 weld metal.

silicates were found along the solidification boundaries. Therefore, the decreased solidification cracking in the primary ferritic weld metal containing high Si and N may be due to the scavenging of S through formation of the high sulfur containing silicates. The formation of the high S containing silicate is also found in the thin foil TEM examination as shown in Figure 10. The type A silicate (SiO_2-MnO) is trapped within the delta ferrite and the high sulfur containing globular silicate (type B) is at dendritic boundary.

It has to be noted that although the nitrogen addition less than 5 vol% to Ar shielding gas appears to decrease hot cracking susceptibility of the high Si (1.25%) fusion zone in type 304, the susceptibility is still significantly greater than that of the low Si (0.54%) weld metal. Therefore, from the hot cracking standpoint, the silicon content should be kept as low as possible (<0.5%).

3.2. Effect of nitrogen in fully austenitic weld metals

The fusion zone hot cracking susceptibility of the fully austenitic type 316 stainless steels as a function of the nitrogen content is shown in Figure 11. It is evident that the hot cracking susceptibility (total crack length) continuously decreases with an increase in the nitrogen content from 0.047% to 0.12%. The maximum crack length reveals that when the nitrogen increased from 0.047 to

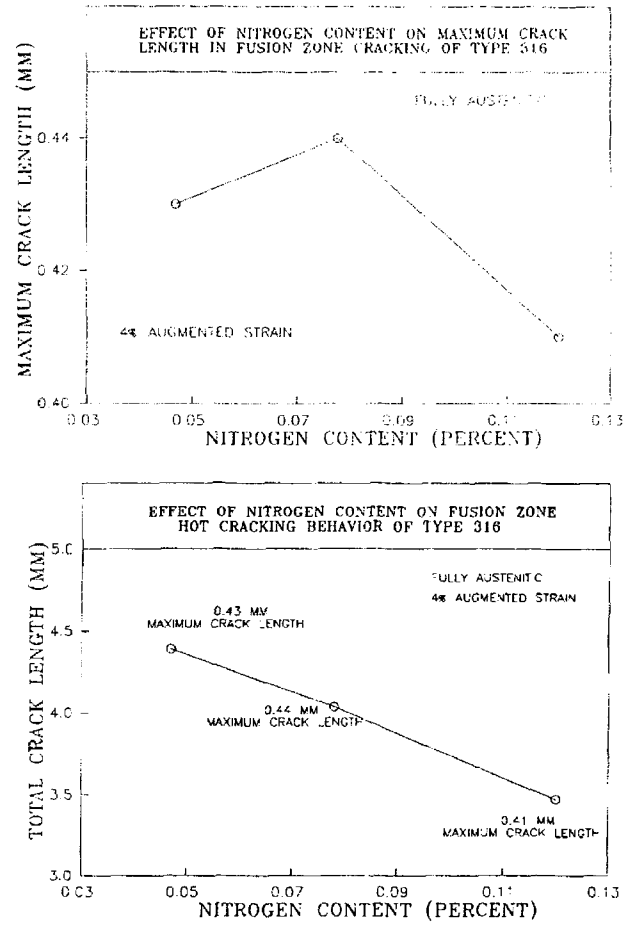

Fig. 11. Effect of N content on solidification cracking in the fully austenitic type 316 stainless steel weld metal.

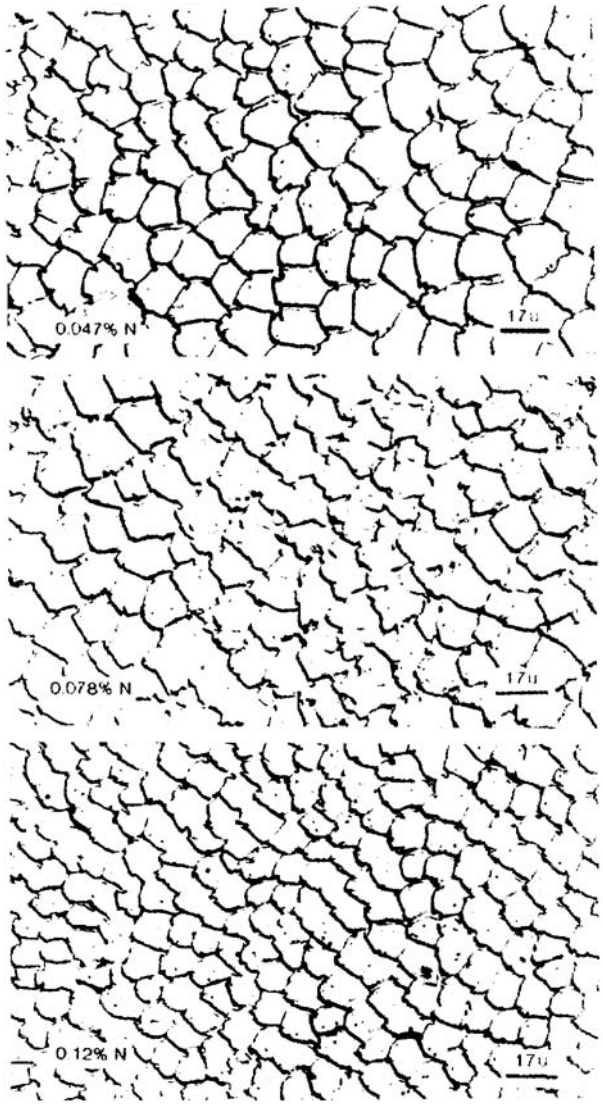

Fig. 12. Typical microstructures in a) 0.047%N, b) 0.078%N and c) 0.12%N containing fully austenitic weld metals.

0.78%, the MCL is almost constant (in fact, slightly increased), but when the nitrogen content further increased to 0.12%, the MCL decreases as is the case for the TCL.

The reasons and mechanisms why the nitrogen addition to the "fully" austenitic weld metal exerts a beneficial effect with regard to solidification cracking are not clear. However, this may be partially related with the cell size in the single phase weld metal. Careful examination of the microstructures from the three weld metals shown in Figure 12 reveals that the highest N (0.12%) containing weld metal appears to have a smaller cellular dendrite size, with no apparent difference in the amount of precipitates in the boundaries. The average

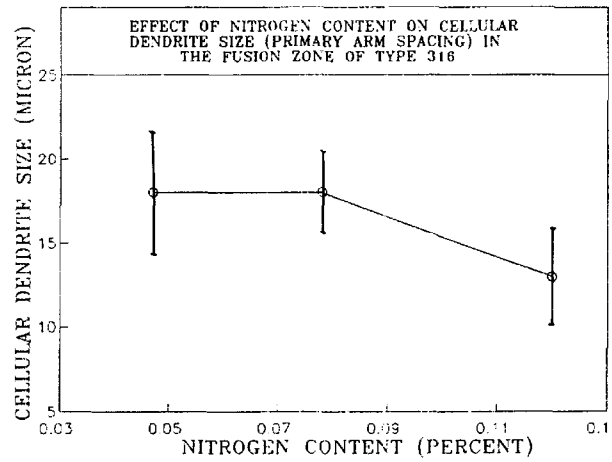

Fig. 13. Influence of nitrogen addition on solidification substructure size.

cell size measured in the five different locations in the fusion zone, as shown in Figure 13, reveals that although there is a significant variation from location to location, the average cell size decreases from approximately 18 μm to 14 μm when the N increases from 0.047% to 0.12%. A similar result was also found by Mundt and Hoffmeister [15, 16] that an addition of 0.6% nitrogen to ferritic weld metal resulted in a fully austenitic weld metal and also refined the cell and grain size. Therefore, the decreased cell size by the N addition may have partially resulted in a reduced cracking susceptibility, because the increased cell boundary area can reduce the concentration of elemental segregation for a given impurities level.

An earlier solidification study [19] showed that the solidification path for fully austenitic weld metal extends away from the Fe corner and generally toward the Cr corner. It also extends in a slightly increasing Ni direction. The three weld metal compositions and the approximate solidification paths are plotted on the liquidus and solidus surface of the ternary Fe-Cr-Ni diagram as given in Figure 14. The isothermal lines are also shown on the diagram. In order to approximate the effect of N, the N content is added to the Ni content by using a factor of 30 according to the Delong method (i.e., Ni+30N). The location of three compositions on the diagram clearly indicates that the liquidus and solidus temperature decreases with an increase in N content when other elements (especially Cr) are maintained constant. As shown previously in the optical microstructures (Figure 12), there was no apparent difference in the amount of second phase precipitates (phosphides and sulfides) in the cell boundaries as a function of nitrogen content.

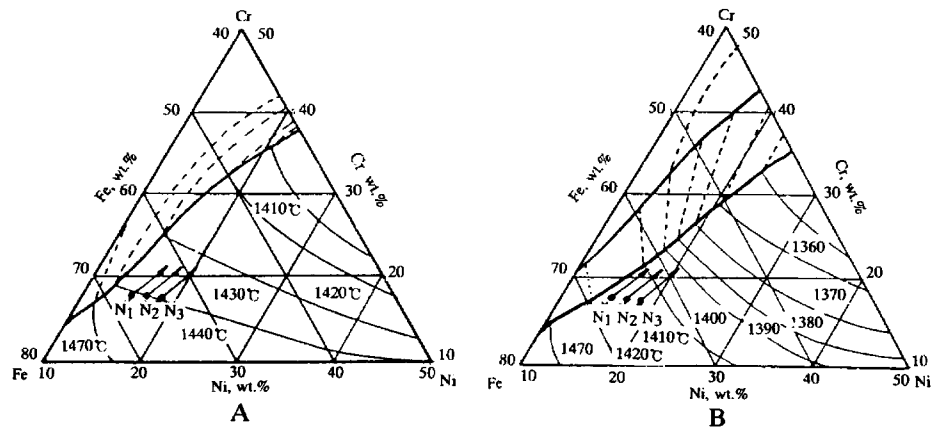

Fig. 14. Approximate solidification paths of 316N-A, 316N-B and 316N-C; a) liquidus and b) solidus surfaces of Fe-Cr-Ni ternary diagram.

Medovar [17] also found that a nitrogen addition to fully austenitic stainless steels does not greatly affect the amount of second phases. Therefore, it can be assumed that the lower temperature limit of the brittleness temperature range (BTR), which is determined by the type and amount of low melting segregates, is constant for the three different N level bearing 316 weld metals. Thus, as shown in the schematic drawing (Figure 15), the BTR becomes narrower as the nitrogen content increases due to the decreased liquidus and solidus temperatures. This may result in a general trend of the decreased maximum crack length (although a deviaton at the midium N content was observed) and the total crack length, in the higher N weld metal.

However, it must be recalled that, although a higher N content decreases the cracking susceptibility of the "fully austenitic" stainless steel weld metal, (when it is compared to that in the primary ferritic weld metal which has the same level of nitrogen), the hot cracking susceptibility of the fully austenitic alloy is still greater than the primary ferritic alloy. Therefore, when alloying with nitrogen to compensate for a lower carbon content, the compositional balance has to be adjusted such that the material solidifies in a primary ferritic mode.

3.3. Effect of rare earth metal (REM)

Two heats of REM modified 347R and 347L were Varestraint tested to evaluate the potential mitigating effect of REM. The 347R has a REM content (0.017%) approximately twice that of 347L (0.008%). Unfortunately, a direct comparison may not be accomplished because of the significant difference in the chemical composition and room temperature ferrite content (and solidification mode) of two heats. The 347L has a fully austenitic solidification mode, while 347R solidifies in a primary ferritic mode and has a 3.5 FN residual ferrite in the (room temperature) microstructure.

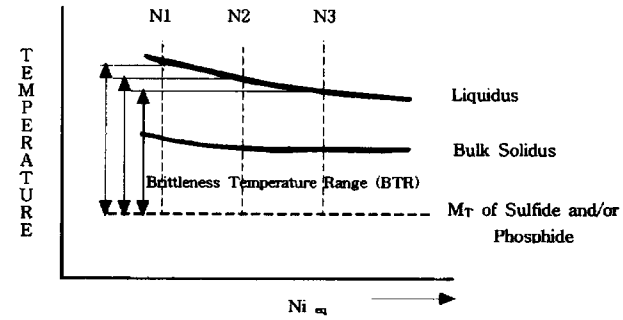

Fig. 15. A schematic Temperature-Ni_{eq} diagram at constant Cr_{eq}, showing the effect of N addition on the BTR of fully austenitic weld metal.

A comparison of solidification cracking susceptibility of 347L and 347R to that of AISI 347, which has a chemical composition almost similar to 347R, is given in Figure 16. This figure clearly indicates that, as may be expected, the small addition of REM (0.008%) in the fully austenitic 347L does not show a beneficial affect on the solidification cracking resistance. The total crack length of 347L is greater than that of 347R and AISI 347 at all augmented strain levels. Matsuda *et al.* [9] have found that optimum level of La to remove S and P as high melting point compounds such as La_2O_2S and LaP in the fully austenitic 310S is approximately; La=4.5P+8.7S. Although they [9] did not give amount of REM required to effectively remove S+P, they found that the REM has a potential equivalent to La. Thus, the same amount of REM may be required. Therefore, approximately 0.12% REM should be required to tie up S+

P as high melting point sulfides and phosphides in 347L. This may be the reason why the small addition of REM (0.008%) did not influence hot cracking susceptibility. However, it has to be considered that although the P+S in 347L is completely removed by the addition of sufficient REM, the effect of Nb in fully austenitic weld metal should not be ignored.

Earlier studies [18] revealed that solidification cracking and weld metal HAZ liquation cracking of type 347 stainless steel were mainly dependent on the Nb content relative to the C and N content instead of the absolute amount of Nb. When the ratio (0.5Nb/(30C+50N)) is greater than about 0.1, the weld metal is susceptible to solidification cracking regardless of the solidification mode and ferrite content. 347L has the ratio of 0.17 which is considered to be high from the solidification cracking standpoint as found in the earlier studies [18].

347R has a significantly high Nb relative to C and N contents. The 0.5Nb/(30C+50N) ratio is 1.23 which is highest among the 347 lots evaluated in this study. Based on the earlier results [18], this heat should have a greater susceptibility to solidification cracking. However, the hot cracking susceptibility of the 0.017% REM containing 347R is lower than AISI 347 and superior to that of the low REM (0.008%) fully austenitic 347L. Therefore, the 0.017% REM must have played a role in the reduction of susceptibility. There is no available data in the open literature regarding what level of REM is required to effectively scavenge the P+S in the primary ferritic weld metal, as opposed to the case of fully austenitic alloy. However, the REM requirement should be less than that required for a fully austenitic stainless steel, because a primary ferritic solidification mode of 347R provides a reduced extent of S and P segregation. Thus, the 0.017% REM may be effectively scavenge the residual S and P, resulting in a reduced susceptibility to solidification cracking.

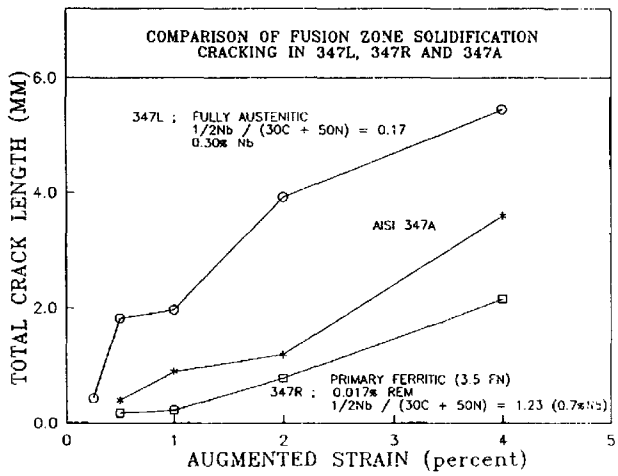

Fig. 16. A comparison of solidification cracking behavior of REM containing 347L and 347R with that of AISI 347.

The typical fusion zone microstuctures for both 347L and 347R are shown in Figures 17 and 18. The microstucture of 347L clearly reveals that the dark appearance microconstituents precipitate more or less continuously along the solidification boundaries. Higher magnification of the constituents from the carbon extraction replica in Figure 17b shows that these microconstituents have a feathery/eutectic lamellar structure, revealing that, as expected, these are Nb(C,N)-austenite eutectics. 347R in Figure 18 shows a duplex ferrite-austenite microstructure indicating a primary ferritic solidification, and the Nb(C,N) and Nb(C,N)-austenite eutectics precipitate less continuously along the interdendritic boundaries. There is no evidence of precipitates of the high melting point sulfides (rare earth oxy-sulfide or rare earth sulfide) or phosphides (rare earth phosphide) in the microstructure because those were re-

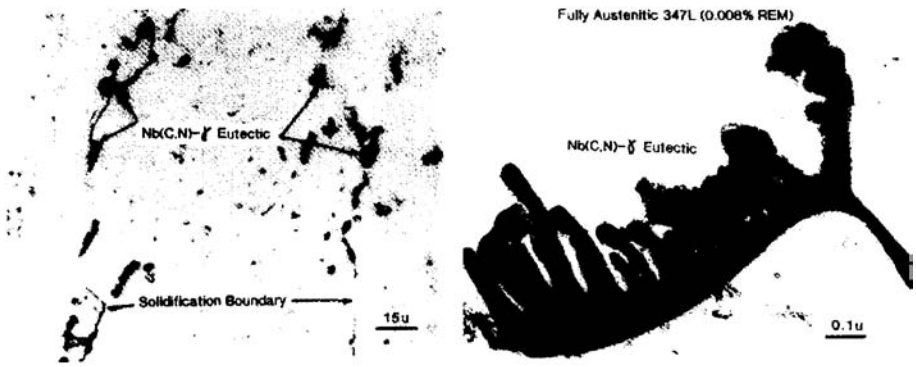

Fig. 17. Typical fusion zone microstructures in the REM (0.008%) containing fully austenitic 347L: a) optical micrograph and b) TEM micrograph showing Nb(C,N)-austenite eutectic.

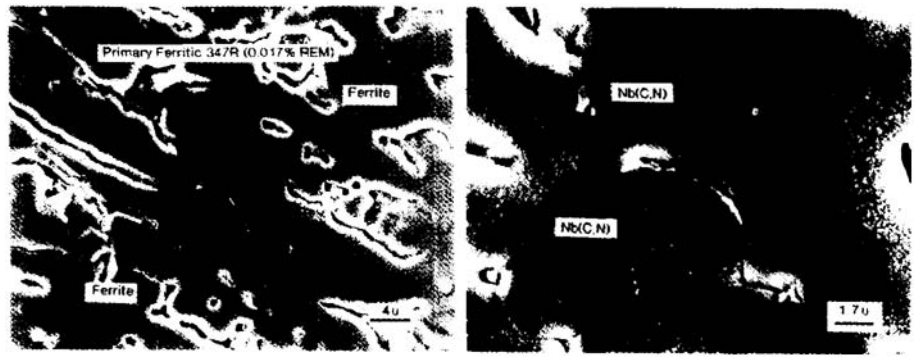

Fig. 18. Typical fusion zone microstructures in the REM (0.017%) containing primary ferritic 347R.

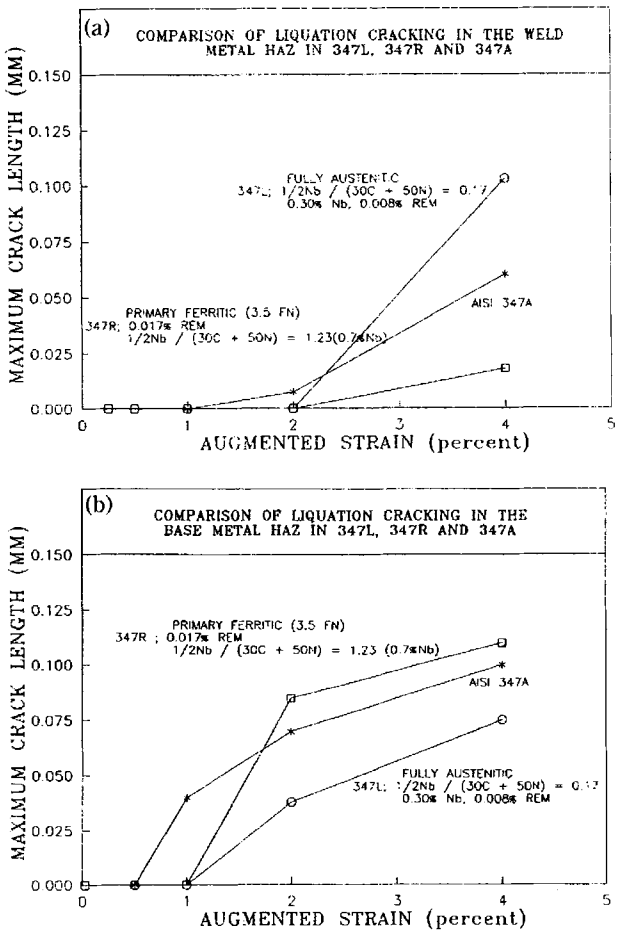

Fig. 19. Comparison of liquation cracking in a) weld metal HAZ and b) base metal HAZ.

moved from the weld metal to the surface as slag during solidificatiion.

The weld metal and base metal HAZ liquation cracking susceptibilities of 347L, 347R and AISI 347 are compared in Figure 19. Liquation cracking susceptibility in the weld metal HAZ of 347L and 347R is similar to the fusion zone solidification cracking susceptibility. Here again, the primary solidification mode is the predominant factor such that the primary austenitic 347L has the greatest crack susceptibility among the three alloys. The addition of 0.017% REM to the primary ferritic 347 seems to have a beneficial effect on the weld metal HAZ liquation cracking as was the case of fusion zone solidification cracking. However, the base metal HAZ hot cracking does not follow the same trend. The lowest Nb containing 347L has a better resistance than the higher Nb containing 347R and AISI 347. At 4% strain, 347L with the lowest Nb and smallest 0.5Nb/(30C+50N) ratio has the lowest base metal HAZ cracking susceptibility. This fact seems to indicate that the REM addition may not influence constitutional liquation and melting of segregated grain boundaries, which are directly responsible for the HAZ liquation cracking. That is, the REM may scavenge the "harmful" elements (P+S) only during solidification. Therefore, when considering the hot cracking behavior in all three weld zones, the reduction of the Nb, P and S contents appears to be the best practice, although a small addition of REM to the primary ferritic weld metal shows a beneficial influence.

4. CONCLUSIONS

(1) While maintaining a primary ferritic solidification mode, a nitrogen addition of 5 vol % in the Ar shielding decreased fusion zone solidification cracking for the high Si (1.25%) fusion zone. However, when the nitrogen addition was increased to 20 vol%, such that the solidification mode changed from primary ferrite to austenite, the fusion zone cracking susceptibility increased significantly.

(2) The decreased solidification cracking susceptibility in primary ferritic high Si and N containing weld metal may be due to a scavenging of S and thus reduced low

melting sulfide formation along the grain/dendrite boundaries (by the formation of high sulfur containing manganese-silicates).

(3) For fully austenitic 316 stainless steel welds, solidification cracking sensitivity decreased with an increase in nitrogen content from 0.047% to 0.12%.

(4) The decreased solidification cracking in the high nitrogen containing fully austenitic 316 weld metals may be due to a decreased solidification cell size. The reduced BTR due to the decrease in the liquidus and solidus isotherms (by increasing N content) may also contribute to the reduced cracking susceptibility of the fully austenitic weld metal.

(5) The addition of REM to 347 stainless steel appears to have a beneficial effect on weld metal solidification cracking and weld metal HAZ liquation cracking, provided the weld metal solidifies in a primary ferritic mode. However, REM addition was found to be ineffective for reducing liquation cracking in the base metal HAZ.

REFERENCES

1. S. Polgary, *Metal Construction,* **1**(2), 93 (1969).
2. T. Orawa and E. Tsunetomi, *Welding Journal,* **61**(3), 82 (1982).
3. C. P. Chou and P. S. Wu, in *Advances in Welding Science and Technology,* (eds., S. A. David), ASM International (1986).
4. W. G. Wilson, D. A. R. Kay, and A. Vahed, in *The Use of Thermodynamics and Phase Equilibria To Predict The Behavior of the Rare Earth Elements in Steel,* p. 132, TMS-AIME, Warrendale, PA (1974).
5. W. G. Wilson, *Journal of Metals,* 14, (1974).
6. V. N. Likhanosov and N. M. Sytnik, *Automatic Welding,* 42 (1985).
7. W. G. Wilson and A. Mclean, in *Desulfurization of Iron and Steel, and Sulfide Shape Control,* The Iron and Steel Society of AIME (1980).
8. N. Morishige, M. Kuribayashi and H. Okabayashi, *IHI Engineering Review,* **15**(2), 1 (1984)
9. F. Matsuda, H. Nakagawa, S. Katayma and Y. Arata, *Transactions of JWRI,* **11**(1), 79 (1982).
10. C. D. Lundin, C. H. Lee, R. Menon and V. Osorio, in *Welding Research, The State of The Art* (eds., by E. Nippes and D. J. Ball), ASM, Metals Park, OH (1985).
11. N. I. Kakhhovskii, *Avt. Svarka,* **8**, 11 (1971).
12. N. P. Zhitnikov, *Svar. Proiz,* **3**, 14 (1981).
13. V. I. Prosvirin, *Problems of the Physical Metallurgy of Austenitic Steels,* **52**, Moscow, Mashgiz (1952).
14. V. M. Zabolotskii, *Welding,* **12**, Leningrad, Sudostroenie (1969).
15. R. Mundt and H. Hoffmeister, in *Stainless Steel '84,* p. 315, Institute of Metals, London (1984).
16. H. Hoffmeister and R. Mundt, *Schweissen und Schneiden,* E198 (1981).
17. B. I. Medovar, *The Welding of High Temperature Steels and Alloys,* Mashinostroenie, Moscow (1966).
18. C. D. Lundin, C. H. Lee and C. Y. P. Qiao, *Development of Hot Ductility and HAZ Hot Cracking Assessment Criteria,* to be published in Welding Journal.